University of Groningen

Bundle-Centric Visualization of Compound Digraphs

Telea, A. ; Ersoy, O.

Published in:
Proceedings ASCI

IMPORTANT NOTE: You are advised to consult the publisher's version (publisher's PDF) if you wish to cite from it. Please check the document version below.

Document Version
Early version, also known as pre-print

Publication date:
2010

[Link to publication in University of Groningen/UMCG research database](#)

Citation for published version (APA):
Telea, A., & Ersoy, O. (2010). Bundle-Centric Visualization of Compound Digraphs. In *Proceedings ASCI*

Bundle-Centric Visualization of Compound Digraphs

A. Telea   O. Ersoy

Johann Bernoulli Institute,
University of Groningen, The Netherlands

Abstract

We present a new approach aimed at understanding the structure of connections in edge-bundling layouts. We combine the advantages of edge bundles with a bundle-centric simplified visual representation of a graph's structure. For this, we first compute a hierarchical edge clustering of a given graph layout which groups similar edges together. Next, we render clusters at a user-selected level of detail using a new image-based technique that combines distance-based splatting and shape skeletonization. The overall result displays a given graph as a small set of overlapping shaded edge bundles. Luminance, saturation, hue, and shading encode edge density, edge types, and edge similarity. Finally, we add brushing and a new type of semantic lens to help navigation where local structures overlap. We illustrate the proposed method on several real-world graph datasets.

1 Introduction

Graphs are used to represent entity-relationship datasets in many application areas, such as network analysis, software understanding, life sciences, and the world wide web. Many visualization methods exist for large graphs, such as scalable node-link diagrams, matrix plots [24], and combinations of the two [10]. Node-link diagrams are often considered more intuitive, and are arguably the most popular [9].

However, node-link layouts can produce significant visual clutter, which shows up as overlapping edges or nodes. Clutter impairs tasks such as finding the nodes that a given edge (or edge set) connect, and at a higher level, understanding the coarse-scale graph structure.

Several approaches exist to reduce clutter in graph visualizations for the above, and similar, tasks. First, the graph can be simplified prior to visualization, *e.g.* by extracting structures such as spanning trees or strongly connected components. Secondly, the layout of nodes and/or edges can be adjusted. Both methods can be applied globally, based on clutter estimation metrics, or locally, based *e.g.* on user interaction [29, 28].

When node positions encode information, they should not be changed. Also, clutter is related most often to edge crossings [18, 11]. Recent research targets clutter reduction and structure emphasis by geometrically grouping, or bundling, edges that follow close paths. Edge-bundling layouts (EBLs) exist for general graphs [6, 13, 17], circular layouts [8], hierarchical digraphs [12], and parallel coordinates [16, 30]

In this paper, we approach the goal of visualizing the coarse-scale structure of an EBL and clarifying edge clutter caused by bundle overlaps. Given a bundling layout, which we do not change, we hierarchically cluster edges seen as similar from the viewpoint of the layout and, optionally, underlying attribute data. Next, we construct simple shapes that encode both geometric attributes of clusters (form, position, topology) and underlying edge data (spatial density and attributes). We render these shapes with an image-based technique that maps their attributes to shading and color on one or more scales. While keeping EBL advantages, our simplified visualization clarifies coarse-scale bundle overlaps by explicitly drawing each bundle as a separate shape, and assists the task of finding nodes connected by a bundle. The simplification level is user controlled. Finally, we add interaction to further clarify overlaps in desired areas and to offer details on demand.

This paper is structured as follows. Section 2 reviews related methods. Section 3 details our technique. Section 4 presents several results. Section 5 discusses our proposal. Section 6 concludes the paper with future work directions.

2 Related work

Reducing edge clutter can be approached by different types of methods, as follows.

1. Edge bundling layouts (EBLs) spatially group edges $e_i \in E$ for a graph $G(V,E)$ using a metric $d(e_i, e_j)$ that models closeness in either graph space, layout space, or both. Edges $e_i = \{p_{ij}\}_{j=1}^{N}$, where $N = |e_i|$, are discretized into points p_{ij} which are positioned so as to minimize d. In hierarchical edge bundles (HEBs) d reflects closeness of edge end-nodes in a hierarchy associated with G [12]. In force-directed bundling (FDB), d models geometric proximity of edge points p_{ij}, and is minimized by a self-organizing approach [13]. Flow

maps hierarchically cluster nodes and edges in a flow graph and yield bundles that emphasize source-sink routes [17]. Geometry-based edge bundling groups edges using a control mesh generated by edge clustering [6]. Parallel coordinates use a metric d that encodes curvature and geometric distance to bundle edges [30].

Overall, EBLs trade clutter for *overlap*. Similar edges are routed close to, or atop of, each other, so less individual edges may be visible. Coarse graph structure becomes visible, but visually disambiguating close or overlapping bundles, *i.e.* seeing nodes these connect, can be hard [8, 14]. Bundles are typically implicit: it is hard to exactly say which are the main bundles in an EBL and what sub-graphs these relate, since bundles do not have a distinct visual identity.

2. Image-based techniques avoid edge clutter by not explicitly rendering edges. Graph splatting convolves nodes and (optionally) edges of a node-link layout with a Gaussian filter [26] into a height or intensity map. Dense edge regions, which can cause clutter in node-link renderings, show up as compact high-value splats. The filter width controls the scale at which overlap is perceived. However producing simplified views, splatting makes it hard to follow edges. Also, the filter width needs careful tuning to avoid creating disconnected, thus misleading, splats.

Shaded cushions are effective for showing hierarchies, and have been used for rectangular and Voronoi treemaps [27, 4] and icicle plots and edge bundles [22]. However, we are not aware of cushions and EBL combinations for more general graphs.

3. Graph simplification techniques replace substructures by simpler ones, or wholly eliminate them, if not essential for the task at hand [1, 3, 25]. This reduces overlap and also emphasizes the overall graph structure. Graph clustering identifies similar sub-structures which can next be simplified. Simplification is not restricted to a unique hierarchy. For example, GrouseFlocks allows users to interactively explore a set of alternative hierarchical simplifications on large graphs, as well as adapt the simplification level, or 'cut' in the hierarchy, dynamically to parts of the graph [2]. A recent review of clustering techniques is given in [20]. In this paper, we use edge clustering, a subclass of graph clustering, to identify and separate edge bundles. However, we do not explicitly simplify the input graph.

3 Method

We aim to simplify a bundled edge visualization by emphasizing the coarse-level bundle structure to help users to visually trace such bundles to the nodes they connect. For this, we make bundles a first-class visualization object using splatting and shaded cushions, hence the name of our method: Image-Based Edge Bundles (IBEB). We use a six-step approach, as follows (see also Fig. 1).

1. We apply a given edge bundling layout (Sec. 3.1).

2. We explicitly group laid out edges into a cluster hierarchy, using a distance that reflects edge positions and data attributes (Sec. 3.2).

3. We choose a set of clusters from the hierarchy at a user-selected level of detail. For each cluster, we create a compact shape around its edges (Sec. 3.3).

4. For each shape, we construct a cushion-like shading profile that also encodes data attributes (Sec. 3.4).

5. We render all shapes in a suitable order to minimize occlusion (Sec. 3.5).

6. We add a new semantic lens method to help visual exploration (Sec. 3.6).

These steps are detailed next.

3.1 Layout

We start with an edge bundling layout $L : G \rightarrow \mathbb{R}^2$ for the input graph $G(V, E)$. The next steps (Sec. 3.2 and further) are fully independent from this layout. The only assumptions made are that

1. each edge $e_i \in E$ is mapped to a set of points $p_{ij} \in \mathbb{R}^2$; different edges can have different amounts of points;

2. the layout does create edge bundles;

As an example, we use the HEB layout [12]. Yet, we use absolutely no hierarchical information beyond the layout. Other bundling layouts can be readily used (Sec. 4).

3.2 Clustering

As a pre-processing step to produce our simplified visualization, we explicitly group related edges. Each edge $e = \{p_j\}_{j=1}^{|e|}$ is modeled as a feature vector $v = \{x_1, y_1, \ldots, x_N, y_N, t_1, \ldots, t_T\} \in \mathbb{R}^{2N+T}$. The first $2N$ elements of v are regularly sampled points along the polyline $\{p_j\}$. N should be large enough to capture complex edge shapes. $N \in [50, 100]$ gives good results on different EBLs and datasets, in line with [13, 12, 8]. Some layouts do not encode semantic edge similarity into positions (assumption 2, Sec. 3.1): The HEB groups edges solely on their ends' hierarchy position; the FDB uses solely edge points' positions. In some cases, *e.g.* visualizing a software system graph, we want to distinguish edge types (*e.g.* inheritance, call, uses) [14]. To separate edges of different types $t \in \mathbb{N}$, we add $v_{2N+1} = t$. Multiple type dimensions can be encoded in $t_1, \ldots, t_T$, although so far we have used a single type component ($T = 1$).

Next, we cluster all edges e_i with a well-known clustering framework for gene data [15]. Intuitively, we replace genes by our vectors v. We have tested several algorithms: Hierarchical bottom-up agglomerative (HBA) using full, centroid, single, and average linkage; and k-means clustering, both with Euclidean and statistical correlation (Pearson, Spearman's rank, Kendall's τ) distances. HBA with average or full linkage and
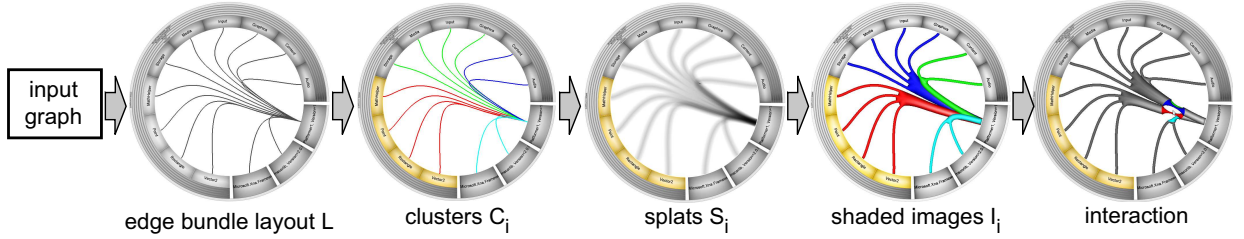
Figure 1: Image-based edge bundle (IBEB) visualization pipeline

Euclidean distance $d(v,w) = \sum_{i=1}^{N+T} \|v_i - w_i\|^2$ give the best results, *i.e.* clusters with edges being close both geometrically and type-wise. To keep edges of different types separated, we bias $t_j \in v$ with a large value $k = \max_{e,e' \in E} \sum_{i=1}^{N} d(e,e')$. Similar techniques are used to handle gene components with different semantics, which also allows users to set weights to the different feature vector components [15].

HBA delivers a dendrogram $T = \{C\}$ with the edge set E as leaves and distances $d(C)$ decreasing from root to leaves. We now select a partition $P = \{C_i\}$ of E so that $\bigcap_{C_i, C_j \in P} = \emptyset$ and $\bigcup_{C_i \in P} = E$. For example, a similarity-based P contains all clusters with a $d(C) < d_{user}$ below a user-given value. Larger d_{user} values give more numerous, and more similar, clusters. Smaller d_{user} values give less, more dissimilar, clusters. Other methods can be used, *e.g.* select P for a given cluster count.

We stress that the clustering method choice is not the core of this paper, but only a tool to create explicit edge groups. Any clustering can be used, as long as it groups edges logically related from an application viewpoint *and* spatially close. Also, it is very important to note that our partition is just a single level, or 'cut', in the graph, which we subsequently visualize.

3.3   Shape construction

Given a user-selected partition P (Sec. 3.2), we now construct a shape to visualize each edge set $C = \{e_i\} \in P$. Due to bundling *and* clustering, edges E typically follow a small set of directions (paths). We use splatting to show bundles in a compact way (Fig. 3). We convolve each edge $e \in C$ with a kernel k which linearly decreases from a maximum K to zero at a distance δ from the edge, and accumulate results, similar to [26]. For this, we sample k in a 64x64 pixels alpha texture and additively blend textured polygons along all $p_i \in e \in C$ (GL_SRC_ALPHA, GL_ONE). We tried both radial and linear profiles for k (Fig. 3 bottom-right). Radial profiles are splatted centered at p_i. Linear profiles are splatted on two polygon strips built by offsetting edge segments $p_i p_{i+1}$ in vertex normal directions $\mathbf{n}_i, -\mathbf{n}_i$ with δ, like stream ribbons in flow visualization. Linear profiles are better: they allow freely choosing the edge resolution (number of p_i) and splat size δ, while these values must be carefully tuned for radial profiles to avoid splatting gaps.

Splatting yields an edge density $D(x) = \sum_{p \in e, e \in C} k(p - x)$ (Fig. 2 b). Next, we threshold

D to obtain a binary shape I (Fig. 2 c)

$$I(x) = \begin{cases} 1, & D(x) \geq \tau \\ 0, & D(x) < \tau \end{cases} \qquad (1)$$

For illustration simplicity, Fig. 2 shows a single cluster (the tree root). In practice, we create one shape I_i for each cluster C_i in the user-selected partition P. Each I_i is, by construction, compact, and surrounds the edge bundle(s) in C_i, with a maximal offset $\delta(K - \tau)/K$. In practice, we always set $\tau = 0.7K$ and $K = 0.2$. δ is user-controlled, ranging between 1% and 5% of the viewport (see Sec. 3.4).

Additionally, we modulate δ to thin shapes half-way between their ends. For this, we use, at each point $p_i, i \in [1,N]$, a value $\delta_i = \delta\left(\varepsilon \left|\frac{i-N/2}{N/2}\right| + 1 - \varepsilon\right)$, *i.e.* shrink shapes from δ at their ends to $(1-\varepsilon)\delta$ in the middle. Good values for ε range around 0.5, which was used for the examples in this paper. Shrinking reduces bundle overlaps, as we shall see next in Sec. 3.5.
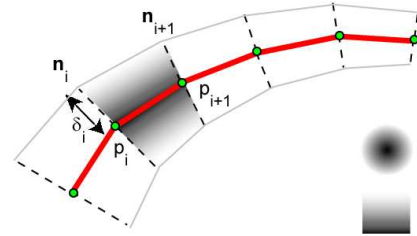

Figure 3: Splatting algorithm details

3.4   Shading

For each binary image I created from clustered edge bundles, we now create a shaded shape that compactly conveys the underlying bundle structure. Following the original bundle metaphor, we want to encode several aspects in a shape:

- *bundling:* The shape should suggest the branching structure of a set of bundled curves in a simplified way;

- *structure:* Finer-level groups of edges, or even individual edges, should be visible;

- *density:* High edge-density regions should be visible. These are cues for strong couplings, relevant to many applications;

- *data:* The shape should be able to encode bundle attributes, *e.g.* edge types.
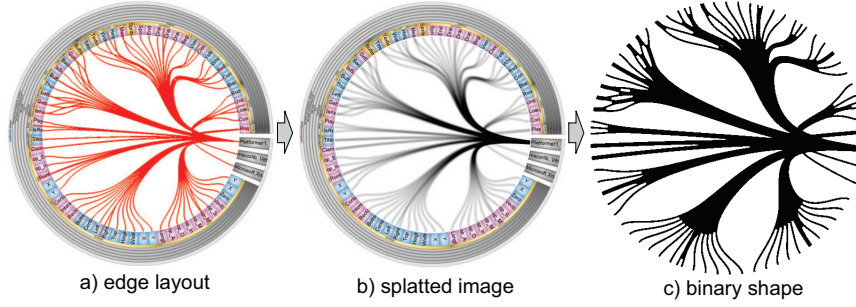
Figure 2: Shape construction. Edge bundles (a) are splatted into a density image (b), next thresholded into a binary shape (c).

For this, we generalize rectangular shaded cushions [27] to our more complex shapes I, as follows. We compute the skeleton $Sk(I)$ of each shape I. $Sk(I)$ is a 1D structure locally centered with respect to the shape's boundary ∂I

$$Sk(I) = \{x \in I | \exists p \in \partial I, q \in \partial I, p \neq q, \|x-p\| = \|x-q\|\}$$

Next, we compute a shading profile

$$H = \frac{1}{2}\left[\min\left(\frac{DT(\partial I)}{DT(Sk)}, 1\right) + \max\left(1 - \frac{DT(Sk)}{DT(\partial I)}, 0\right)\right] \tag{2}$$

where $DT(\partial I)$ and $DT(Sk)$ are the distance transforms of the boundary ∂I and skeleton Sk respectively. We compute both DT and Sk using the implementation described in [23]. For any shape topology or geometry, H smoothly varies between 0 on ∂I and 1 on $Sk(I)$, as shown for a different application in [19]. Figure 4 b,c show Sk and H (the latter on a blue-to-red colormap) of the shape given by splatting Fig. 4 a.

We now set the hue, saturation, value, and transparency h, s, v, a at each pixel of I using the profile H, splatting density D (Sec. 3.3), and edge types, following the aims listed earlier in this section. We set $v = H^\alpha$, with $\alpha = 0.5$. This darkens shapes close to their border and brightens them close to the skeleton. The factor 0.5 smooths out H (Eqn. 2), creating a look akin to classical shaded cushions [27]. Next, we map edge types to hue h. Two options were explored: each shape has a different hue, or hues map edge types. The second option is relevant when clusters contain only same-type edges (Sec. 3.2). Finally, we use s and a to create different visual styles (Table 1).

The *convex* style renders opaque shapes dark and saturated at the border and bright and white in the middle (Fig. 4 d). In contrast to Phong shading H as a true height signal, as in [27, 5], this style emphasizes the skeletal structure (branching pattern). We see now the effect of the splat size δ (Sec. 3.3). Higher values yield thicker, simpler shapes (Fig. 4 d). Smaller values yield thinner shapes with individual edges better visible (Fig. 4 e). We can further emphasize a bundle's branching structure by using $\max[0, (H - H_{min})/(1 - H_{min})]$ instead of H in Table 1. H's isolines continuously change from the shape's boundary to its skeleton, being halfway at $H = 0.5$ (see Fig. 4 c and [19]). $H_{min} = 0.5$ yields shapes which are thinner and also further emphasize the bundle structure, as in Fig. 4 f.

Style	s	a
Convex	1-H	1
Density-luminance	$1 - HD$	1
Density-saturation	HD	1
Cores	H	$1 - H^3$
Outline	0	$1 - HD$

Table 1: Shape shading styles (see Secs. 3.4, 3.5)

The last four shading styles in Table 1 are effective when visualizing several clusters, as discussed next.

3.5 Rendering

For a given clustering partition P, we now render one shape I for each cluster in back to front order, *i.e.* sorted on shape size (foreground pixel count $|I|$). Placing small shapes in front of larger ones reduces occlusions and makes small bundles visible. Figure 5 illustrates this. Image (a) shows a dependency graph of 419 nodes and 988 relations extracted from a C# software system, laid out with the HEB. Nodes are .NET assemblies, packages, classes, and methods. Several bundles show up, but it is hard to determine (even with interaction) which subsystems they connect. Overlaps make it hard to visually follow a bundle end-to-end. Image (b) shows the result of our method, on a level-of-detail with 18 clusters, using the convex style (Sec. 3.4). For illustration only, clusters were given different random hues from a handcrafted colormap. Using a gray rather than white background emphasizes the coarse-scale bundles. Image (c) shows the density-luminance style (Table 1). Brightness emphasizes clusters with many edges. Figure 5 d serves the same goal, but uses saturation: High-density areas are colorful, low-density areas are gray. Image (d) shows the *cores* style. Areas close to bundle skeletons are opaque, the rest is transparent. This reduces overlaps and stresses graph structural aspects, similar in aims to the opacity bands in clustered parallel coordinates [7].

Figure 5 f shows the *outline* style. Here, we modulate alpha, to create transparent outlined tubes (Table 1). To reduce clutter caused by transparency, we use grayscale images. Although less salient than the previous styles, outlines are an useful visual cue of overall structure, especially when combined with interaction techniques.

Finally, we explored the possibility to add more visual detail to a bundle. For a user-chosen level d_{min} and
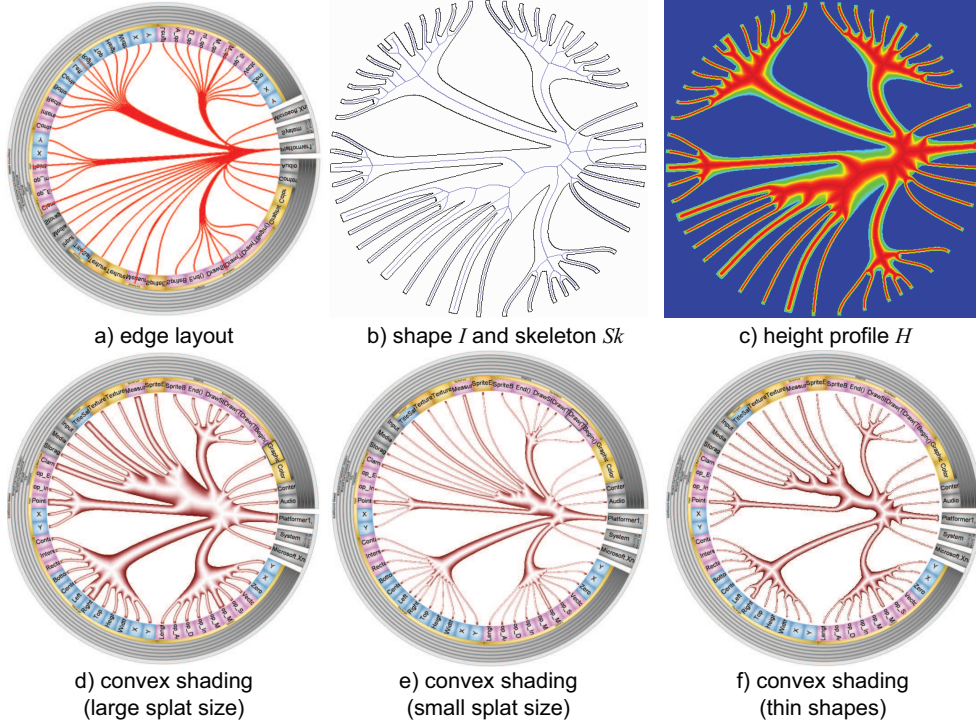
Figure 4: Shading pipeline (Sec. 3.4). Edges in a cluster (a) and their binary shape *I* and skeleton *Sk* (b) and shading profile *H* (c). Convex shading with shape thickness as function of the splat size (d,e) and shading profile thresholding (f)

partition $P = \{C\}$, we first compute H as in Sec. 3.4. Next, we re-partition C (Sec. 3.2) for a higher $d'_{min} = \mu d_{min}$, where $\mu = 1.2$ gives good results. Third, we add the profiles H' of each C' in its refined partition P'_i, scaled to a lower range $[0,h]$, to the coarse-scale H_i. We normalize the result $H + \sum_{C' \in P'} hH'$ and use it for shading (Sec. 3.4). Finer-scale bundles create luminance ridges within their parent clusters. From discussions with the users, we noted that bi-level images are perceived as more suggestive than single-level ones, as the second level acts as a detail texture suggesting the bundled edges, and also eliminate the undesired luminance peaks created by skeleton branches reaching to the corners of the bundle shapes (compare Figs. 5 (c) and (e)). However, our thin and long shapes preclude adding more levels to actually show bundle hierarchies like *e.g.* in cushion treemaps.

3.6 Interaction

By construction, EBLs favor edge overlaps (Sec. 2), so occlusion cannot be fully avoided. We alleviate this by several interaction techniques. First, we use classical brushing to render pixel-thin edges in the shape under the mouse. This shows the nodes linked by a given bundle, even if only a small part of the bundle is visible. Clicking on a shape brings it to front, sends it to back, or hides it. This helps bringing bundles of interest into focus.

We add a new interaction tool to further explore overlapping bundles: the digging lens. Given a focus point x (the mouse pointer), and a pixel p within the lens radius R, $\|p - x\| < R$, we upper threshold the profiles $H(p)$

with $H_{min} = t[1 - (\|p - x\|/R)^2]$ for all visible shapes, where $t = 0.8$ gives the maximal thinning in the lens center. This smoothly shrinks shapes closer to the lens center, along the idea shown in Fig. 4 f (Sec. 3.4). We set the shapes' saturation to 1 in the lens and 0 outside. As the lens moves, shapes inside it get thinner (thus have less overlap) and also colorful (thus easy to focus on without distraction from outside shapes). As the user moves the mouse inside the lens, we automatically bring to front the shapes touched by the mouse. Figure 6 shows the digging lens. At the thin circle location (a), we see bundle overlaps. This cue triggers further exploration. For example, we want to see what is behind the blue bundle (A, inset). Activating the lens (by pressing Control) shows eight clusters, made distinct by shrinking and coloring (b). Moving the mouse over *e.g.* the red bundle (B, see inset) brings it to front, so we now see that it connects the node groups N_1, N_2 and N_3 (c). The entire process takes a few seconds and requires one key and one mouse click. Although useful, the digging lens cannot fully handle all possible overlaps: Where long bundles of same thickness overlap nearly completely, the lens will shrink them equally, and thus not reveal the hidden bundles. The lens is effective in places where bundles overlap but have slightly different directions and/or thicknesses.

4 Results

Figure 7 shows the IBEB applied to the software dependency graph from Sec. 3.5. As a use-case, we consider analyzing *type usage*, *i.e.* inheriting from a class or using its type (functionality) in client code. This is one
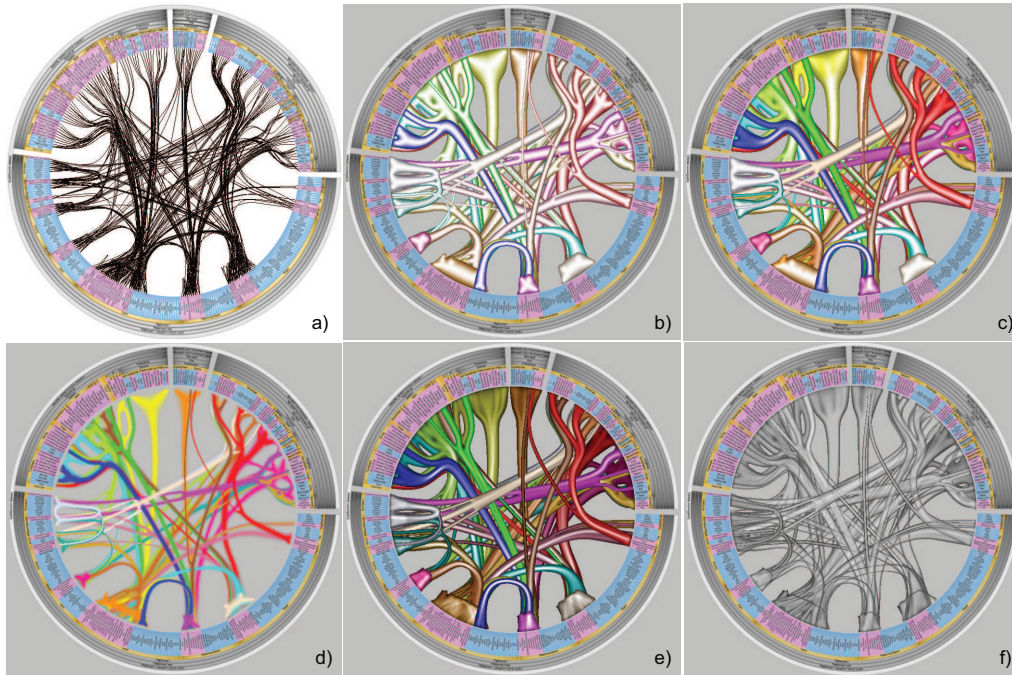
Figure 5: Rendering styles: convex shapes (b), density-luminance (c), density-saturation (d), bi-level (e), and outlines (f).
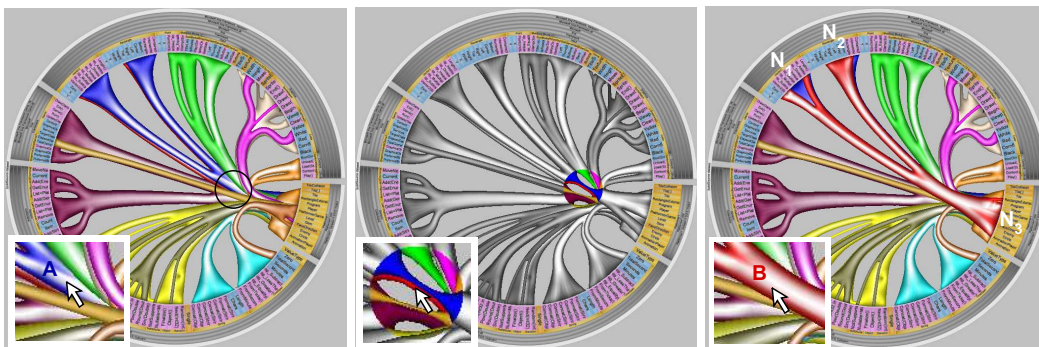

Figure 6: The digging lens is used to interactively explore areas where shapes overlap. Insets show zoomed-in details.

of the hardest kinds of dependencies to refactor in software. To analyze different coupling types, we first use the HEB with type-colored edges (calls=yellow, class member reads/writes=blue, type usage=red) (Fig. 7 a). We see a thick red bundle that links subsystems A and B. However, without iterative node selection, we cannot see which *parts* of A connect to which *parts* of B. Also, edge color blending makes it hard to see edge types at overlaps (arrow in the figure).

Next, we use the IBEB with convex shading and bi-level rendering (Fig. 7 b). Clusters contain only same-type edges (Sec. 3.2) and are colored on this type. We see now that member read/write relations form localized bundles not extending across classes (small light blue bumps, see *e.g.* the light blue arrow in (b)). This is a good sign for information hiding. Also, two red bundles appear. With two clicks, we bring these to front (b). We now see two separate subsystems in A connected to two separate subsystems in B. For illustration, we click on one of the two bundles (A_1B_1) and change its color to blue (Fig. 7 c). We have now split the original red bundle into two relation sets: A_1B_1 and A_2B_2. Fig. 7 d

shows further insight in the clustering: all bundles colored with different hues and overlaid with the actual pixel-thin edges. Albeit brief for space limitations, this example illustrates one main point: Classical edge bundles, like HEB, effectively show coarse-scale subsystem connections, but do not expose the finer-scale coupling structure within bundles. IBEB further reveals this structure, by showing where actual edges that 'enter' the bundle will 'exit'.

To further understand the IBEB strong and weak points, we performed a formative user study. Twenty 3rd year CS students at the Univ. of Groningen, the Netherlands, were given the IBEB implemented atop of a software analysis tool using the HEB [21]. The tool imports dependency graphs (inheritance, class field usage, function calls, and containment hierarchy) from Visual C++, .NET/C#, and Java. The C# software discussed earlier was provided by the tool developers as an interesting use-case. Participants were asked to find dependencies between several indicated modules; list the four most important call and field usage paths in the system; and comment on the overall system modularity. Search, fil-
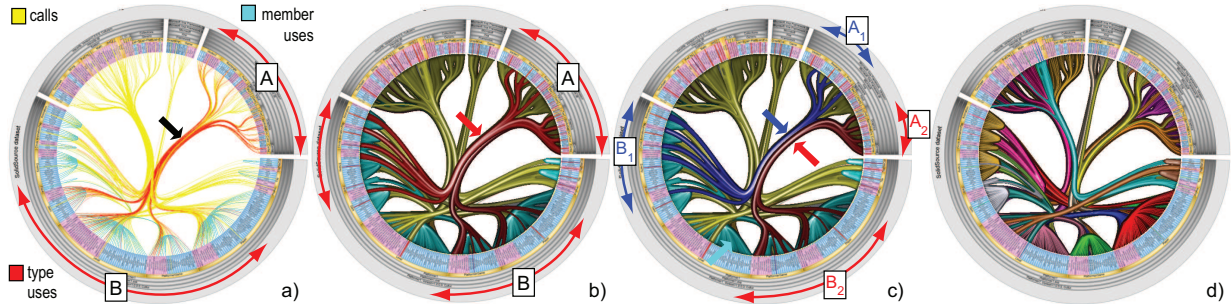
Figure 7: Software dependency graph exploration with IBEB (see Sec. 4)

ter, and node selection (available in the original tool) were disabled, so the tasks had to be completed mainly focusing on edges. One week was given to familiarize with the tool (which has a detailed manual) and execute the tasks. Effective usage time was 5 to 8 hours. The images in Fig. 7 come from this study.

Besides the actual answers, the following points were mentioned by all users (except two who did not complete the study):

- Classical HEB is very effective when (a) there are few bundle overlaps, or (b) one does not need to visually determine which *parts* of a large bundle go to which specific node groups;
- Although overlap exists, IBEB reveals several end-to-end (node-to-node) coarse-scale bundles which are not visible with classical HEB;
- The digging lens is effective in locally unraveling occluded bundles at a location of interest;
- The IBEB has an 'organic' look which is pleasing and invites exploration.

Overall, the IBEB combines the advantages of HEB with an easier understanding of *dense* bundles. In the traditional HEB, a thick, dense, bundle is seen as such but one cannot directly see whether there is finer-level structure, *e.g.* the bundle actually consists of several sub-bundles which connect different node groups, like in Fig. 7. This can be done by a trial-and-error selection of individual nodes to see if their edges indeed pass through the bundle of interest. Such selection is easily done in the HEB, but harder in layouts that draw nodes as small points, *e.g.* the FDB. In contrast, IBEB makes bundles explicit, and individually, visible, so users can easier relate bundles to the nodes they connect. The fact that IBEB shows less fine-scale detail than the HEB does not seem to be a major problem, as individual edges are mainly explored once one has decided which few node(s) one wants to inspect. When this is known, both the HEB and IBEB are equally effective - in IBEB, brushing over a node and/or bundle highlights its edges, drawn as individual lines, just like in the HEB. For the several selection and brushing features we support, we refer to [21].

Our users also mentioned several desirable additions. First, although shading and back-to-front rendering were seen as effective, overlaps still exist. The digging lens helps to analyze overlaps, but only locally.

Secondly, edge direction cues are required. We tried several methods for this, *e.g.* luminance or saturation modulation of our bundle shapes, but this was found to darken images too much. Further work in this area is needed.

5 Discussion

We next discuss some technical aspects of our method.

Performance: We ran the IBEB, implemented in C++ and OpenGL 1.1, on several systems running Windows Vista/XP, 1.5 to 3.5 GHz, and 2 GB to 4 GB RAM. The clustering used [15] handles 10 to 20K edges in under 0.1 seconds. Splatting, shading, rendering, and interaction (OpenGL-based) run in real-time on consumer graphics cards.

Visual metaphor: The IBEB *convex* rendering style resembles the shaded edge bundles in illustrative parallel coordinates (IPC) [16], with some differences. Our shapes have a much higher variability, depending on the EBL used. We use hierarchical agglomerative clustering, while IPC uses *k*-means. We use skeletons in shading to emphasize the bundles' branching structure, to reduce overlaps (shrink shapes globally or locally by the digging lens), and for the *cores* rendering style. IPC uses different shapes and a shading style that mainly emphasizes line density.

Scalability: The IBEB's main limitation is *visual* scalability. Using 10 to 30 shapes shows the coarse graph structure. More shapes create too many overlaps. However, we aim to provide a simplified view, not a full-blown replacement for bundled edges.

Acknowledgements

We are grateful to Dennie Reniers and Lucian Voinea for the code of the SolidSX tool [21], datasets, and use-cases, and to Danny Holten for the force-directed bundling layout data (Sec. 4) and many insightful comments.

6 Conclusions

We have presented an image-based simplified visualization for edge bundles (IBEB). Given a layout that creates spatially close edge bundles, we visualize bundles using shaded overlapping compact shapes. We reduce

the visual complexity of classical bundle visualizations, emphasize coarse-scale structure, and help navigating from bundles to the connected nodes. We make bundle overlaps explicit, and add interaction to locally disambiguate these. Level-of-detail techniques help to select the visualization granularity and further explore overlaps.

Many extensions are possible. Different shading and edge clustering strategies can be used to address additional use cases, *e.g.* emphasize connections of particular types and/or topologies in a graph. New techniques can be designed to convey additional edge data such as direction or metrics atop of our metaphor. Finally, the IBEB can be extended to other fields, such as flow or tensor visualization. We plan to explore these avenues in future work.

References

[1] J. Abello, F. van Ham, and N. Krishnan. ASK-graphview: A large scale graph visualization system. *IEEE TVCG*, 12(5):872–880, 2006.

[2] D. Archambault, T. Munzner, and D. Auber. GrouseFlocks: Steerable exploration of graph hierarchy space. *IEEE TVCG*, 14(4):900–913, 2008.

[3] D. Auber, Y. Chricota, F. Jourdan, and G. Melancon. Multiscale visualization of small world networks. In *Proc. IEEE InfoVis*, pages 75–81, 2003.

[4] M. Balzer, O. Deussen, and C. Lewerentz. Voronoi treemaps for the visualization of software metrics. In *Proc. ACM SOFTVIS*, pages 165–172, 2005.

[5] D. Bruls, C. Huizing, and J. J. van Wijk. Squarified treemaps. In *Proc. IEEE VisSym*, pages 33–42, 2000.

[6] W. Cui, H. Zhou, H. Qu, P. Wong, and X. Li. Geometry-based edge clustering for graph visualization. *IEEE TVCG*, 14(6):1277–1284, 2008.

[7] Y. Fua, O. Ward, and E. Rundensteiner. Hierarchical parallel coordinates for exploration of large datasets. In *Proc. IEEE Visualization*, pages 43–50, 1999.

[8] W. Gansner and Y. Koren. Improved circular layouts. In *Proc. GD*, pages 386–398. Springer, 2006.

[9] M. Ghoniem, J. D. Fekete, and P. Castagnola. A comparison of the readability of graphs using node-link and matrix-based representations. In *Proc. IEEE InfoVis*, pages 17–24, 2004.

[10] N. Henry and J. D. Fekete. NodeTrix: A hybrid visualization of social networks. *IEEE TVCG*, 13(6):1302–1309, 2007.

[11] I. Herman, G. Melancon, and S. Marshall. Graph visualization and navigation in information visualization: a survey. *IEEE TVCG*, 6(1):24–43, 2000.

[12] D. Holten. Hierarchical edge bundles: visualization of adjacency relations in hierarchical data. *IEEE TVCG*, pages 741–748, 2006.

[13] D. Holten and J. J. van Wijk. Force-directed bundling for graph visualization. *Comp. Graph. Forum*, 28(3):983–990, 2009.

[14] H. Hoogendorp, O. Ersoy, D. Reniers, and A. Telea. Extraction and visualization of call dependencies for large C/C+ code bases: A comparative study. In *Proc. IEEE VISSOFT*, pages 45–53, 2009.

[15] M. D. Hoon, S. Imoto, J. Nolan, and S. Miyano. Open source clustering software. *Bioinformatics*, 20(9):1453–1454, 2004.

[16] K. McDonnell and K. Mueller. Illustrative parallel coordinates. *Comp. Graph. Forum*, 27(3):1031–1038, 2008.

[17] D. Phan, L. Xiao, R. Yer, P. Hanrahan, and T. Winograd. Flow map layout. In *Proc. IEEE InfoVis*, pages 219–224, 2005.

[18] H. Purchase. Which aesthetic has the greatest effect on human understanding? In *Proc. GD*, pages 248–261, 1997.

[19] M. Rumpf and A. Telea. A continuous skeletonization method based on level sets. In *Proc. IEEE VisSym*, pages 151–160, 2002.

[20] S. Schaeffer. Graph clustering. *Comp. Sci. Review*, 1:27–64, 2007.

[21] SolidSource. SolidSX software explorer, 2009. www.solidsourceit.com/products/SolidSX-source-code-dependency-analysis.html.

[22] A. Telea and D. Auber. Code Flows: visualizing structural evolution of source code. *Comp. Graph. Forum*, 27(3):831–838, 2008.

[23] A. Telea and J. J. van Wijk. An augmented fast marching method for computing skeletons and centerlines. In *Proc. IEEE VisSym*, pages 251–258, 2002.

[24] F. van Ham. Using multilevel call matrices in large software projects. In *Proc. IEEE InfoVis*, pages 227–232, 2003.

[25] F. van Ham and M. Wattenberg. Centrality based visualization of small world graphs. *Comp. Graph. Forum*, 27(3):975–982, 2008.

[26] R. van Liere and W. de Leeuw. Graphsplatting: Visualizing graphs as continuous fields. *IEEE TVCG*, pages 206–212, 2003.

[27] J. J. van Wijk and H. van de Wetering. Cushion treemaps: Visualization of hierarchical information. In *Proc. IEEE InfoVis*, pages 73–80, 1999.

[28] N. Wong and S. Carpendale. Using edge plucking for interactive graph exploration. In *Proc. IEEE InfoVis (poster comp.)*, pages 51–52, 2005.

[29] N. Wong, S. Carpendale, and S. Greenberg. EdgeLens: An interactive method for managing edge congestion in graphs. In *Proc. IEEE InfoVis*, pages 51–58, 2003.

[30] H. Zhou, X. Yuan, H. Qu, W. Cui, and B. Chen. Visual clustering in parallel coordinates. *Comp. Graph. Forum*, 27(3):1047–1054, 2008.